Available online at www.sciencedirect.com
ScienceDirect
International Journal of Heat and Mass Transfer 51 (2008) 2346–2360
International Journal of HEAT and MASS TRANSFER
www.elsevier.com/locate/ijhmt

Heat transfer augmentation along the tube wall of a louvered fin heat exchanger using practical delta winglets

Michael J. Lawson *, Karen A. Thole

Mechanical and Nuclear Engineering Department, The Pennsylvania State University, University Park, PA 16802, United States

Received 16 March 2007; received in revised form 14 August 2007
Available online 23 October 2007

Abstract

Delta winglets are known to induce the formation of streamwise vortices and increase heat transfer between a working fluid and the surface on which the winglets are placed. This study investigates the use of delta winglets to augment heat transfer on the tube surface of louvered fin heat exchangers. It is shown that delta winglets placed on louvered fins produce augmentations in heat transfer along the tube wall as high as 47% with a corresponding increase of 19% in pressure losses. Manufacturing constraints are considered in this study whereby piercings in the louvered fins resulting from stamping the winglets into the louvered fins are simulated. Comparisons of measured heat transfer coefficients with and without piercings indicate that piercings reduce average heat transfer augmentations, but significant increases still occur with respect to no winglets present.
© 2007 Elsevier Ltd. All rights reserved.

Keywords: Compact heat exchanger; Vortex generator; Louvered fins

1. Introduction

In the automotive industry, decreasing the size of compact heat exchangers is of great importance for fuel economy. Advantages to decreasing heat exchanger size include weight savings, as well as a reduction in the required frontal area of a vehicle that must be dedicated to the heat exchanger. Louvered fin heat exchangers are commonly used over continuous fin heat exchanger designs in automotive applications because of the substantial advantages they provide in heat transfer performance, while causing acceptable increases in pressure losses. Increases in efficiency allow for louvered fin heat exchangers to be smaller and lighter, while providing the same heat transfer capacity. Fig. 1 shows a compact louvered fin heat exchanger that is typical of those used by the automotive industry.

Louvers increase heat transfer by disrupting thermal boundary layer formation along the fin, causing a significant decrease in airside thermal resistance, which comprises 85% of overall resistance to heat transfer. There have been several studies, summarized by Chang et al. [1,2], that have attempted to determine an optimal louver pattern to maximize heat transfer. To date however, there has been little research performed that investigates the possibility of fundamentally altering the louvered fin geometry to improve heat transfer on the tube wall surface. Approximately 15% of total heat transfer takes place on the tube wall surface. Even so, by improving tube wall heat transfer efficiency, significant increases in heat exchanger performance can be realized. For example, increasing the heat transfer along the tube wall by 50% corresponds to a 7.5% increase in overall heat transfer for the heat exchanger.

Recent studies by Lawson et al. [3], Sanders and Thole [4], and Sanders [5] have identified one possible alteration that may be a practical means for improving louvered fin heat exchanger performance. The implementation of delta winglets, shown in Fig. 2, into louvered fin geometry was

* Corresponding author. Tel.: +1 814 863 0174.
E-mail address: mlawson@psu.edu (M.J. Lawson).

0017-9310/$ - see front matter © 2007 Elsevier Ltd. All rights reserved.
doi:10.1016/j.ijheatmasstransfer.2007.08.016

Nomenclature

b	two times winglet height
c	winglet chord
D_H	hydraulic diameter
f	fanning friction factor
f_0	baseline fanning friction factor
F_d	fin depth
F_h	fin height
F_p	fin pitch
h	convection coefficient, $h = (q''_{total} - q''_{cond} - q''_{rad})/(T_w - T_{in})$
k_{air}	thermal conductivity of air
K_c	loss coefficient for sudden contraction of flow entering louvered array
K_e	loss coefficient for sudden expansion of flow leaving louvered array
L_l	louver length
L_p	louver pitch
Nu	Nusselt number, $Nu = hL_p/k$
Nu_0	baseline Nusselt number
q''_{cond}	heat flux lost by conduction through instrumented wall
q''_{total}	applied heat flux at heated wall
q''_{rad}	heat flux lost by radiation from the heated wall
Re	Reynolds number based on louver pitch, $Re = U_{ff}L_p/v$
t	louver thickness
t_w	winglet thickness
T_{inlet}	temperature measured at test section inlet
T_w	temperature measured on the heated tube wall
U	local velocity
U_{ff}	mass averaged velocity through the louvered fin array
x	streamwise coordinate through the louver array
X	non-dimensional fin depth, $X = x/F_d$
z	distance of delta winglet from the tube wall
Z	non-dimensional distance of delta winglet from the tube wall, $Z = z/L_p$

Greek symbols

α	winglet angle of attack
Λ	delta winglet aspect ratio, $\Lambda = 2b/c$
θ_L	louver angle
ΔP	pressure drop through louvered fin array
ρ_{air}	density of air
v	kinematic viscosity of air

shown by these past studies to be promising. Louvered fins are manufactured using a stamping process whereby a modification to the geometry would also be stamped out of the same sheet of metal from which the fins are made. Louvered fins that incorporate winglets into their design would therefore have piercings in locations where the winglets were stamped. These piercings were not simulated for many of the configurations presented in the aforementioned studies.

Lawson et al. [3] and Sanders and Thole [4] performed experimental and computational investigations into the effect winglets with and without simulated piercing had on tube wall heat transfer. Lawson et al. [3] and Sanders and Thole [4] used a simplified louvered fin geometry where the louver surface spanned the entire heat exchanger core. Winglets with a thickness of the louvers were shown to have only a small positive effect on heat transfer. Incorporating piercings into the louvered fins was shown to slightly increase heat transfer compared to tests without piercings; however, the maximum winglet augmentation of tube wall heat transfer observed was only 8%.

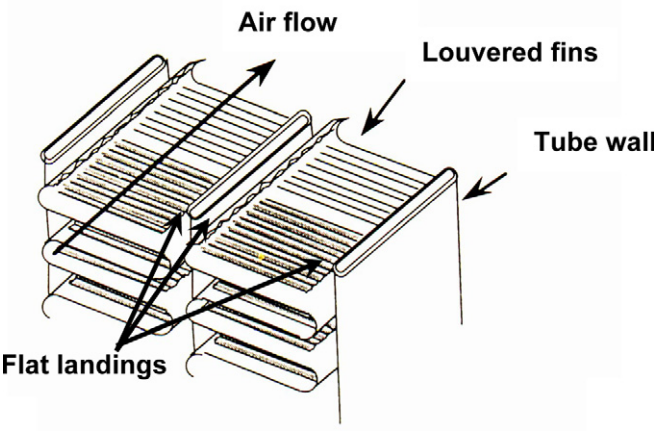

Fig. 1. Louvered fin heat exchanger showing the location of the flat landing along the tube wall.

Sanders [5] later tested the effects of winglets incorporated into a more realistic louvered fin geometry and measured heat transfer augmentation as high as 53% along the tube wall with only a 21% increase in pressure losses. The louvered fin geometry used for this study modeled the transition between the louvers and the tube wall, including the flat landing abutting the tube wall. Alternatively, Sanders [5] did not model the winglet piercings that would be left from manufacturing the winglets.

Currently, no studies have been performed incorporating winglets with simulated piercings into a louvered fin geometry where the flat landings along the tube wall were considered. As will be discussed in the next section, past studies have shown that measurements of tube wall heat transfer made using a simplified louvered fin geometry where the louvers span the test section do not agree with those made using a more realistic geometry that includes the louver-tube wall transition and flat landing. Although Lawson et al. [3] simulated delta winglets with piercings,

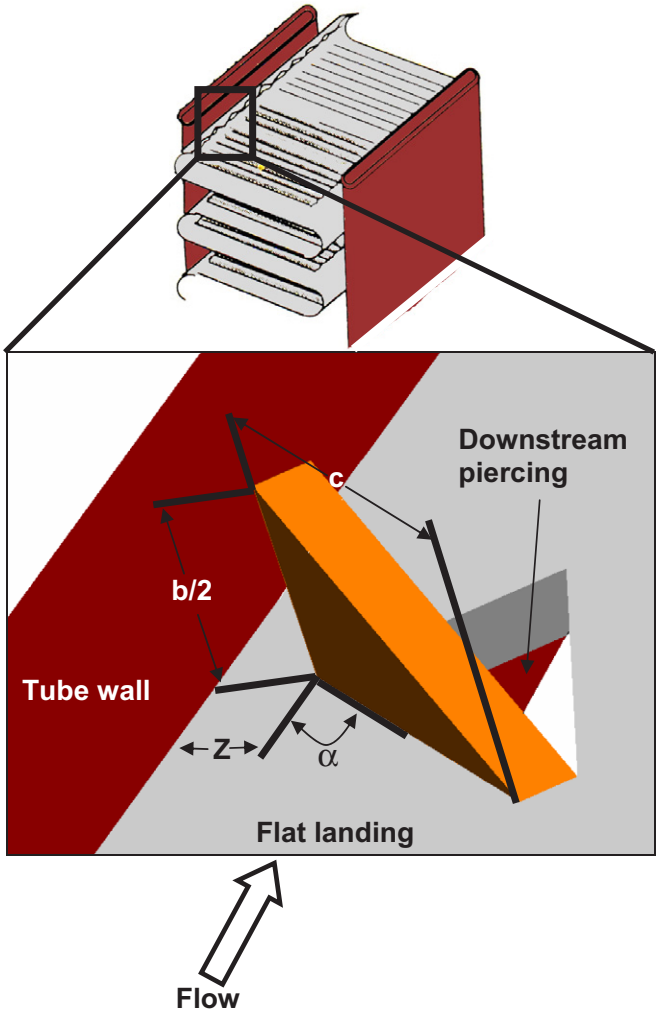

Fig. 2. Diagram of a delta winglet located on the flat landing.

their results can not be used to make direct inferences about winglet performance in a heat exchanger as they modeled louvered fins that spanned the entire height of the fin. This paper continues the work of Lawson et al. [3] and Sanders and Thole [4] by examining the effect of winglets and piercings on tube wall heat transfer for a realistic louvered fin taking into account manufacturing constraints.

2. Past studies of relevance

The majority of research on louvered fin heat exchangers has attempted to determine an optimal geometry for the louvers. Beauvais [6] was one of the first to perform an investigation of louvered fin heat exchangers. He found that louvers not only disturb the flow through the louver array, but also cause the flow to be redirected in the louver direction. Davenport [7] built upon the understanding of louver effects by suggesting that the mechanism by which louvers increase heat transfer performance is the breaking and reforming of the thermal boundary layer. It has since been accepted that this disruption of thermal boundary layer growth is the mechanism by which louvers decrease overall air-side resistance to heat transfer.

Aided by advances in the ability to model complex geometries computationally, detailed performance characteristics of heat exchangers have been studied through the use of computational fluid dynamics. Atkinson et al. [8] modeled two- and three-dimensional louvered fin arrays. They found that accounting for the three-dimensionality of the flow field more accurately matched published experimental results. Tafti and Cui [9] performed a computational study that investigated four different geometries for the transition between louvers and the tube wall. Tafti and Cui [9] found that for a realistic three-dimensional transition geometry, away from the tube wall the flow was mostly two-dimensional, while near the tube wall in the transition region flow was highly three-dimensional. Tafti and Cui's [9] work showed that the transition between the louver and tube wall must be modeled in order to obtain accurate heat transfer measurements in the tube wall region. In their paper, Tafti and Cui [9] suggest that if a method of augmenting tube wall heat transfer can be determined, there is potential for large improvements in overall heat transfer performance.

Delta winglets placed at an angle to a flow are known to create streamwise vortices. Biswas et al. [10] studied the effect of delta winglets on heat transfer over a flat plate. Augmentations as high as 65% were measured on the plate surface. Biswas et al. [10] concluded that delta winglets show significant promise for improving the heat transfer performance of heat exchangers. Gentry and Jacobi [11] studied the effect of delta wing vortex generators placed in developing channel flow and on flat plates. Delta wings should not be confused with delta winglets. While both induce streamwise vortices, the geometries are slightly different. Using delta wings, Gentry and Jacobi [11] measured increases in average channel heat transfer of up to 55% between Reynolds numbers (with respect to channel hydraulic diameter) of 400 and 2000. Interestingly, Gentry and Jacobi's [11] results suggested that vortex strength, and not the location with respect to the channel boundary layer, was the most important factor in enhancing convective effects in the boundary layer. Biswas et al. [10] and Gentry and Jacobi [11] identified that winglet performance and vortex strength improved with increasing angle of attack and Reynolds number.

Recently, the possibility of using inlet vortex generators as a method of increasing overall heat exchanger efficiency has been investigated by Smotrys et al. [12] and Joardar and Jacobi [13]. Both interrupted fin and louvered fin heat exchangers were tested with delta wings placed at the entrance of the arrays. When delta wings were included in the interrupted fin design [12], heat transfer augmentation occurred, but was highly dependent on the number of vortex generators used. For the study of louvered fin arrays [13], delta wings placed at the leading edge caused augmentations up to 23%. Although these studies are

similar to the present research, there is a significant difference in both the vortex generator geometry (delta wings versus delta winglets) and placement in the heat exchanger.

Other computational studies [14,15] have simulated delta winglets in fin-tube heat exchangers and also predicted significant increases in heat transfer. The results showed that as vortices propagate, they increase surface heat transfer in the region downstream of the winglets. One of the only studies that investigated the effect of delta winglets implemented over the length of the heat exchanger, including simulated piercings, was that of Vasudevan et al. [16]. This computational study modeled delta winglets, both with and without simulated piercings, placed in triangular duct flow. Vasudevan et al. [16] predicted that through the use of delta winglets, the required length of a triangular duct heat exchanger could be significantly reduced, possibly by as much as 20%, while maintaining the same heat transfer to the working fluid. It was found that implementing piercings caused both a more complex flow in the channel and some negative effect on overall winglet performance. High augmentations were still observed with piercings and Vasudevan et al. [16] concluded that winglets with piercings are a practical method of augmenting heat transfer performance.

The information contained within this paper reports on the investigation of varying winglet and piercing geometries on heat transfer and pressure drop performance using a 20:1 scaled louvered fin geometry as shown in Fig. 3. Sanders and Thole [4], who used the same testing facility, were the first to consider the possibility of implementing delta winglets along the tube wall surface of a louvered fin heat exchanger. Their work was performed using a simplified heat exchanger geometry where the louvers spanned the full height of the fins with the flat landing along the tube wall being neglected. Tube wall heat transfer augmentation over the baseline case with no winglets was as high as 35% with pressure loss penalties of only 13%. Sanders [5] continued work with delta winglets by placing them on the flat landings along the tube wall surface. Sanders [5] observed significant differences in the heat transfer results obtained using the simplified geometry, confirming that the tube wall transition and flat landing must be modeled to obtain accurate measurements. Convective heat transfer augmentations as large as 53% with a

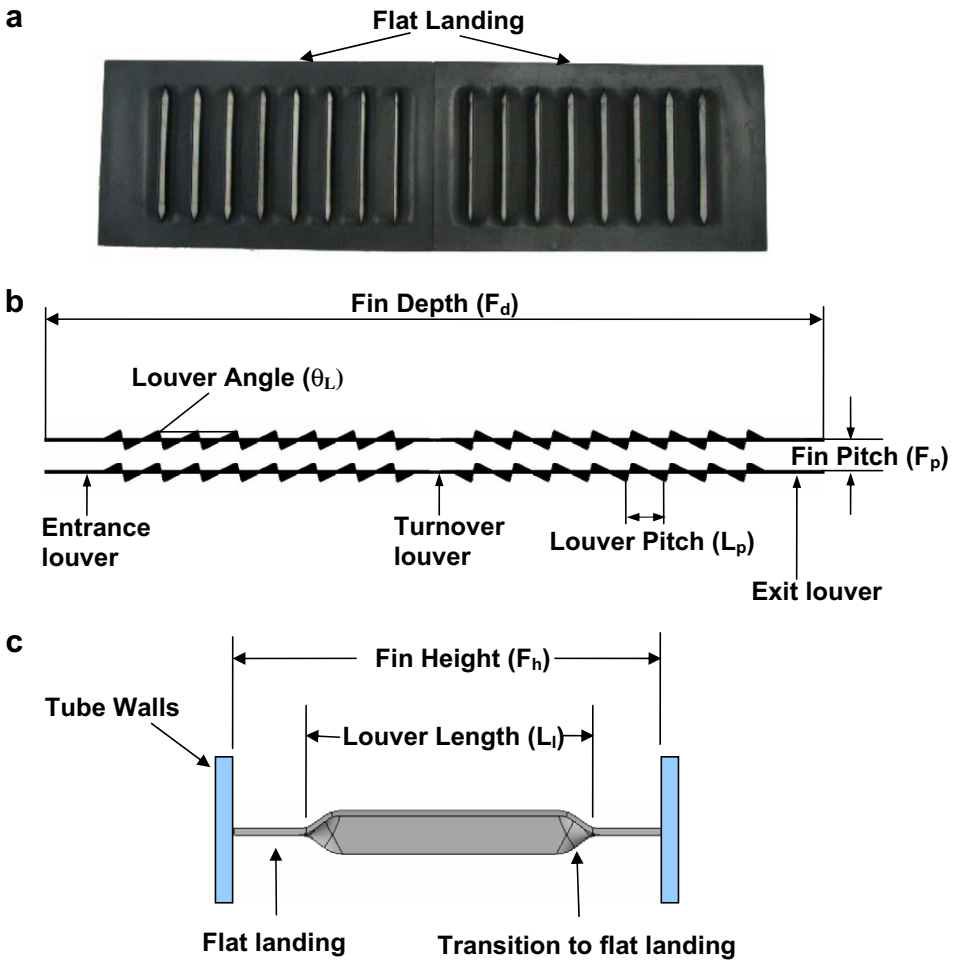

Fig. 3. Louvered fin geometry used for testing: (a) picture of the top view, (b) side view, and (c) front view. Note that the fin was molded in two pieces as seen in (a).

corresponding increase of 21% in pressure losses were measured. Clearly, there is potential for the use of delta winglets as a means of augmenting tube wall heat transfer. Before conclusions can be drawn on their potential benefit in future designs for louvered fin heat exchangers, the effect of piercing on winglet performance needs to be quantified since piercings would be present for louvered fins manufactured incorporating winglets.

3. Louvered fin geometry

The louvered fin geometry used in this study was a 20:1 scale model (to allow for good measurement resolution) from an actual heat exchanger, and was the same as that used by Sanders [5]. This geometry models the louvers, the flat landing, and the transitional region where the two adjoin as shown in Fig. 3. The louver length, including the transitional region from the louver into the flat landing (see Fig. 3), was 70% of the total fin height.

Each fin consisted of 17 louvers, as shown in Fig. 3, which was comprised of an entrance louver, seven louvers, a turnover louver, seven louvers, and then the exit louver. Entrance, turnover, and exit louvers were twice the length of the other louvers and were specifically designed to turn the flow and increase heat transfer coefficients on the louver surfaces. All louvers had a louver angle of 27° with respect to the entrance flow, a louver pitch of 27.9 mm, a fin pitch of $0.76L_p$, a louver thickness of $0.079L_p$, a fin depth of $20L_p$, and a fin height of $5.3L_p$.

4. Winglet and piercing geometries

Several winglet and piercing geometries were tested and compared with baseline testing results. The winglet parameters that were varied included the winglet thickness, aspect ratio, distance from the tube wall, and number of winglets. Fig. 2 illustrates the winglet parameters that were varied during testing.

Winglet aspect ratios were varied between 1.5 and 3. For all tests, the winglet height was maintained at $0.35F_p$. This height was chosen so that the winglets were approximately half of the channel height when taking into account the thickness of the louvered fins (see Fig. 3). Three different winglet distances from the tube wall of $0.15L_p$, $0.22L_p$, and $0.29L_p$ were tested. In addition, two different winglet thicknesses were tested that included thin winglets having a thickness of $0.03t$, as well as realistically thick winglets having a thickness of t. The realistic thickness was representative of a winglet that would result from the stamping process during louvered fin manufacturing.

To allow piercings to be incorporated into the louvered fins, square cutouts were machined into the flat landings. A laser was used to make inserts with piercings that simulated winglet stampings, which fit into the cutouts. Inserts were secured into the cutouts and winglets were placed in the appropriate location. Fig. 4 shows an insert simulating a winglet with a piercing and a louvered fin with cutouts.

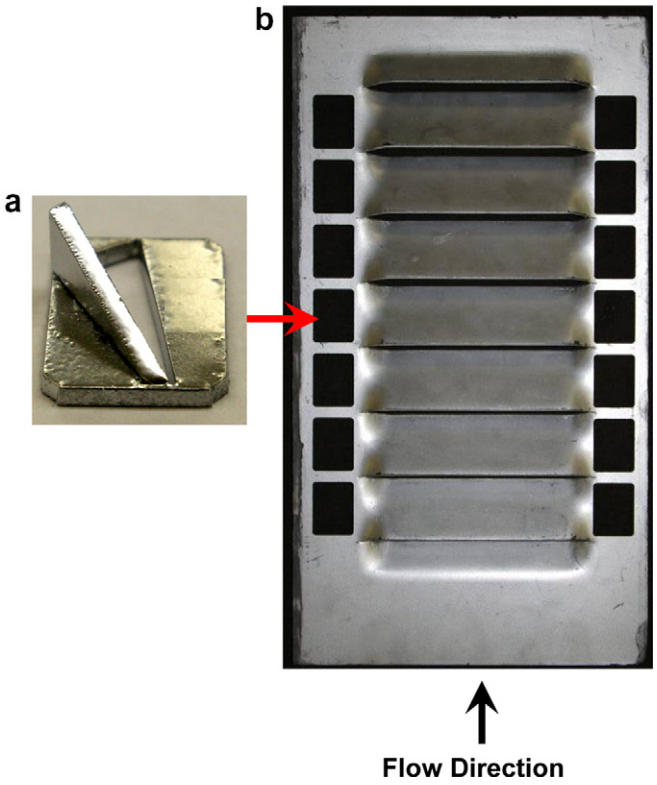

Fig. 4. (a) Plexiglas winglet and insert used to simulate piercings and (b) cutouts milled into a scaled louvered on the flat landing.

Inserts allowed for a range of piercing locations and winglet geometries to be tested. Piercings were only simulated using winglets with a thickness of the louvered fins, as this is the thickness that would result from the stamping process. Winglets angled toward the wall were always simulated with piercings downstream of the winglets and for winglets angled away from the wall, piercings were only simulated on the upstream side. For the remainder of this paper, louvered fins incorporating winglets with no piercings will be referred to as solid louvered fins while louvered fins with winglets and piercings will be referred to as pierced louvered fins.

Experiments were conducted incorporating either 28 or 16 winglets into the louvered fin geometry and were only placed in locations corresponding to the cutouts that are seen in Fig. 4. For tests using 28 winglets, winglets were placed at every cutout location. Tests using 16 winglets had winglets placed at every other cutout location. Sanders and Thole [5] demonstrated little difference in heat transfer performance between winglet configurations having angles of attack of 30° and 40°. Both angles indicated good heat transfer augmentations relative to angles less than 30° for which poor augmentation was observed. For most tests with no piercings, winglets had $\alpha = 40°$. To allow for piercings to fit onto the flat landing, tests incorporating piercings had $\alpha = 30°$.

During assembly of heat exchanger cores, louvered fins are placed in a number of different orientations by those

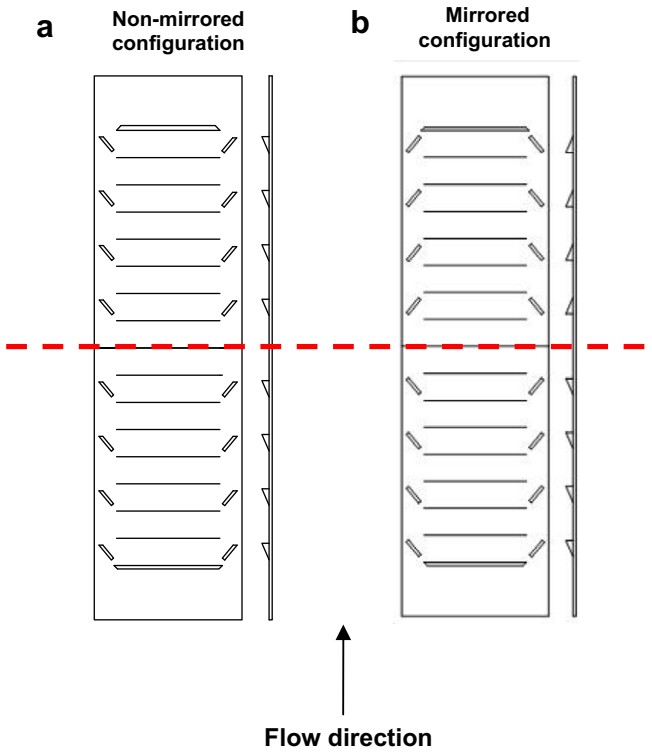

Fig. 5. (a) Mirrored and (b) non-mirrored winglet configurations. The dotted line passing through the turnover louver is the plane across which the winglet setup must be mirrored. (For interpretation of the references in colour in this figure legend, the reader is referred to the web version of this article.)

assembling the core. As such, it is important that the louvered fins perform equally well regardless of flow direction over the fins. For the performance of louvered fins to be independent of flow direction, the winglet and piercing setup should appear the same to the working fluid regardless of flow direction. For this reason, most of the testing performed is for setups that are mirrored (or symmetric) across the turnover louver. Fig. 5 illustrates the difference between mirrored and non-mirrored winglet configurations. If the louvered fin and winglet geometry are mirrored, performance is independent of core orientation during assembly.

5. Experimental facilities and instrumentation

The test rig used for these experiments, shown in Fig. 6, was an open loop channel consisting of an inlet nozzle, test section, laminar flow element, and a motor-controlled blower. Excluding the test section, the experimental facility was the same as that used by Sanders and Thole [4], Ebeling and Thole [18], Lyman et al. [19], and Stephan and Thole [20]. The inlet nozzle was designed using CFD to provide uniform flow at the inlet to the test section, which was verified using a laser Doppler velocimeter. The nozzle consisted of honeycomb screen leading into a 16:1 area contraction. A 1.5 hp motor, controlled with an AC inverter, powered a centrifugal fan which pulled air through the test section. A laminar flow element for measuring the test section flowrate was located between the test section and the blower.

The test section, shown in Fig. 7, was designed to accommodate flow periodicity for the three-dimensionality of the fins. The test section is the same as that designed, built, and used by Sanders [5] in his study using the same louvered fin geometry with twelve louver rows being simulated. This number of rows has been shown by Springer and Thole [21] to be sufficient to allow for periodic flow. The louvered fins were placed in a bounded flow path and were held in by brackets along the side walls, which simulated the tube walls of an actual heat exchanger. The bounding walls on the top and bottom of the test section were designed to simulate natural flow through an infinite louvered fin array. To do so, the top and bottom bounding walls directed flow in the louver region of the fins in the louver direction, while allowing the flow that passed through the channels formed by the flat landings to travel along those landings. The flow path provided by the top and bottom bounding walls can be seen in Fig. 7.

To simulate the hot tube wall of a heat exchanger, a custom, constant heat flux plate using a sandwich of kapton

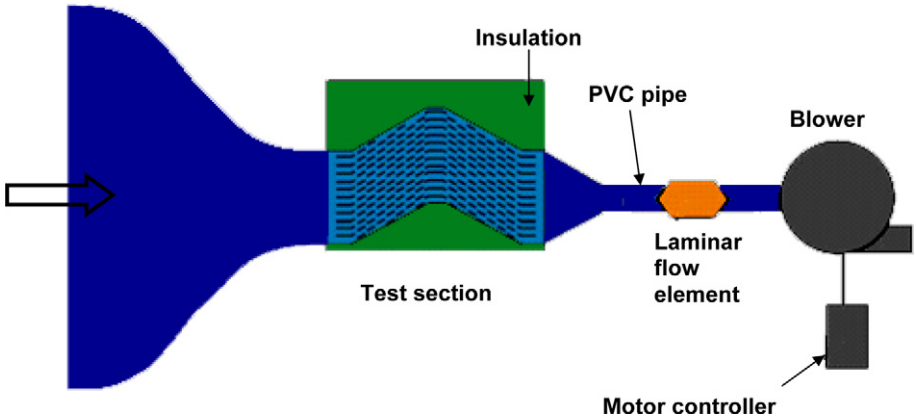

Fig. 6. Schematic of the open loop wind tunnel used for all experiments.

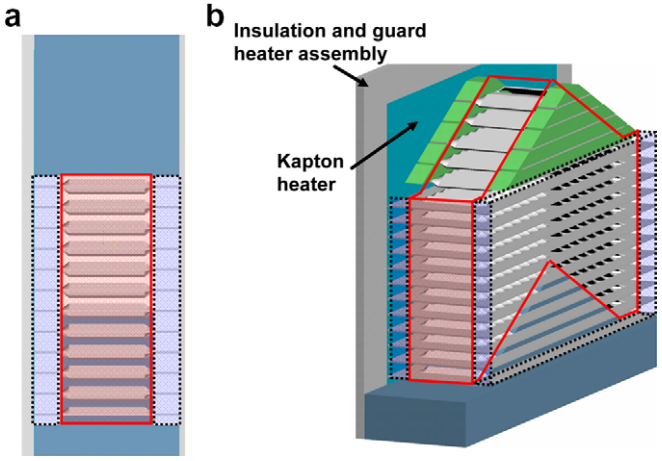

Fig. 7. (a) Front view and (b) isometric view of the test section used. The solid outlined areas indicate the region through which louver-directed flow traveled. The dotted outlined areas indicated the region of flows over the flat landings at the edge of the fins.

and inconel was secured to one of the side walls as shown in Fig. 7. The side of the heater exposed to the test section had a thin copper coating to ensure a constant heat flux surface. The side wall opposite the heater was made of lexan and allowed for visual access to the test section. This wall was not heated, as past studies have shown that the thermal boundary layers from the tube walls do not merge. Therefore to obtain tube wall heat transfer measurements, only one side wall needed to be heated.

As the main purpose of this study was to measure convective heat transfer coefficients along the tube wall, it was important to determine the heat flux on tube wall convected by air passing through the test section. The heat flux produced by the heater was determined by measuring the resistance of the heater and the current passing through it. Conduction losses out the back side of the heated wall were minimized by placing insulating foam behind the heater. A guard heater, illustrated in Fig. 7, was placed behind the foam and the temperature was set to match the temperature of the tube wall heater as closely as possible. Through the use of the foam insulation and guard heater, conduction losses from the back of the test section were typically less than 4% of the total applied heat flux. Another source of heat loss from the tube wall was radiative heat transfer from the copper surface of the kapton heater to the louvered fins. To minimize these losses, fins were painted with a silver paint having an emissivity of 0.3. Radiative losses were typically less than 15% of the applied heat flux.

Twenty type *E* thermocouples were imbedded in the heated tube wall directly behind the heat flux surface. These thermocouples were equally spaced over the length of the louvered fin array in the streamwise direction and were oriented in the center of the channels formed by the flat landings of two fins. To ensure periodic conditions were occurring in the array, thermocouples were placed one channel above and below the thermocouples used for data acquisition to check for periodicity. Tests for heat transfer periodicity in the pitchwise direction indicated less than 4% variation between louver channels. Thermocouples were also placed on the guard heater in locations corresponding to those of the thermocouples imbedded behind the heated side wall. To ensure the accuracy of measurements, at least 200 samples were taken and then averaged. Before Nusselt numbers were calculated, the test rig was allowed to come to steady state, which occurred four hours after the heaters and blower were turned on. Allowing the test rig to run for an additional hour resulted in less than 1% change in average Nusselt number along the heated side wall.

Pressure drop measurements across the louvered fin array were made with a 0–25 Pa pressure transducer. Pressure taps were located $0.73L_p$ upstream and downstream of the louvered fins and were drilled into the lexan wall. The pressure tap located $0.73L_p$ downstream of the array was in the wake region of the louvered fin array. At the Reynolds numbers tested, this wake was very weak. The spatial variation in velocity was determined to have a negligible effect on the static pressure.

Experiments were conducted in an open loop facility and the inlet temperature and pressure varied with room conditions. For all experiments, the temperature at the inlet to the test section was between 18 °C and 23 °C with inlet stagnation pressure ranging between 93 and 97 kPa. Temperature and pressure variations were accounted for in determining the proprieties of air.

Any geometry modification to the heat exchanger must be effective at improving performance over the entire range of operation conditions. Consulting with a heat exchanger manufacturer [17] three representative Reynolds numbers were identified as relevant for testing ($Re = 216$, 577, and 955). All experiments were performed at these Reynolds numbers to determine the effect of delta winglets on heat exchanger thermal performance.

6. Data analysis and uncertainty

Nusselt numbers were calculated by determining the amount of heat convected from the heated side wall by the air passing through the test section. Nusselt numbers were calculated as

$$Nu = \frac{q''_{\text{total}} - q''_{\text{cond}}(X) - q_{\text{rad}}(X)}{[T_{\text{wall}}(X) - T_{\text{inlet}}]} \frac{L_p}{k_{\text{air}}} \quad (1)$$

Radiative heat loss was determined using view factor equations from Modest [22]. Losses from conduction were determined using the measured temperature difference between the guard heater and the tube wall heater. The plastic material from which the fins were made had a low thermal conductivity and the contact area was small such that heat conduction into the fins from the tube wall was negligible. As the tube wall thermal boundary layers do not merge for the louvered fin heat exchanger considered in the study, heat transfer is similar to an interrupted flat plate boundary layer with a constant heat flux. For typical

boundary layer studies, the reference temperature used is the freestream temperature, which is the inlet temperature to the test section.

To quantify winglet performance, Nusselt number augmentations were calculated as a percentage increase over the baseline case having no winglets. Only heat transfer coefficients measured downstream of the first winglet were used to calculate Nusselt number augmentations. Pressure losses for different winglet and piercing setups were characterized by Fanning friction factors, calculated using the equation

$$f = \frac{D_H}{4F_d}\left(\frac{2\Delta P}{U_{ff}^2 \rho_{air}} - K_c - K_e\right) \quad (2)$$

Sudden flow area change as air enters and exits the louvered array were accounted for through loss coefficients K_c and K_e determined from White [23].

Methods described by Moffat [24] were used to calculate uncertainties in Reynolds number, Nusselt numbers, and friction factor. The largest uncertainty in measured Nusselt number occurred at the entrance louver where the temperature difference between the heated side wall and free stream air was at a minimum. At this location Nusselt number uncertainty was as high as 7%. Typically, averaged Nusselt uncertainties were 4%, 4%, and 3% for Reynolds numbers of 216, 577, and 955, respectively. Friction factor uncertainty was 8% at a Reynolds number of 955, and increased with decreasing Reynolds number. Low pressure drops through the test section at the Reynolds number of 216 caused the friction factor uncertainty to be 51%. Because of the high uncertainties associated with pressure drop measurements at Reynolds numbers of 216 and 577, this paper will only use friction factor data measured at Reynolds number 955 to make comparisons between different winglet and piercing geometries.

7. Solid louvered fins with and without flat landings

Comparisons are made in this section of the paper between the simplified louvered fin geometry where no flat landing is modeled [4] and the scaled louvered fins where the flat landing is modeled. Fig. 8 shows measured Nusselt numbers along the tube wall for both louvered fin geometries at $Re = 216$ and 955. As was expected, the Nusselt numbers started high as the leading edge of the tube wall heater initiated the thermal boundary layer, and then decreased as the boundary layer along the tube wall grew. There was a significant difference in measured tube wall Nusselt numbers between the two geometries. While the streamwise-averaged Nusselt numbers were within 1% for the different geometry louvered fins at $Re = 955$, the local data showed significant differences. The most notable difference occurred just after the turnover louver ($X \approx 0.6$) where, for the geometry with no flat landings, a significant increase in Nusselt number was measured with no increase

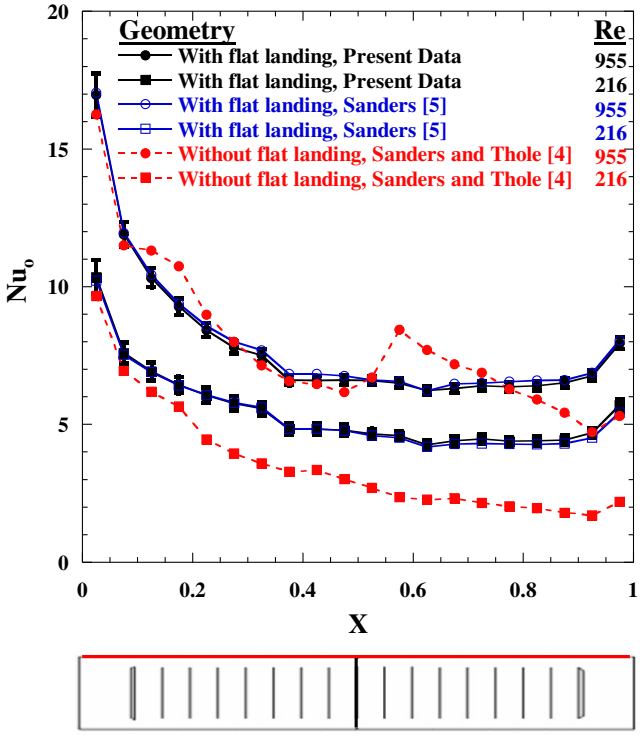

Fig. 8. Heat transfer results for different louvered fin geometries. Also shown are baseline measurements made by Sanders 5 using the same louvered fin geometry with flat landings. $X = 0$ corresponds to the entrance of the louvered fin array. Representative uncertainty bars are shown at each X location for data from the present study.

in Nusselt number for the geometry where the landings were modeled.

Smoke visualization indicated that there were fundamentally different flow fields along the tube wall for the different geometries. Flow through the louvered fin array with no landings was louver-directed near the tube wall as the louver abutted the tube wall. The turnover caused a flow re-direction which led to an increase in Nusselt number downstream of the turnover louver.

Flow through the louvered fin array with flat landings contained two defined flow regimes. Flow passing through the louvered region of the fins became louver-directed, as with the simplified geometry; however, flow along the tube wall where the fin had a flat landing was similar to channel flow which was undisturbed by the louvers. As such, the measurements made using the geometry modeling the flat landings did not show the effect of the turnover louver because of the channel-like flow along the tube wall. While the turnover louver would influence heat transfer on the louver surfaces, the flow disturbances have a minimal effect on heat transfer coefficients along the tube wall. Considering that significantly different flow fields were observed for the different geometries, it was expected that the effect of winglets would also be appreciably different as will be shown in the next sections of this paper.

Measured pressure losses through the louvered fin arrays were converted to friction factors, which allowed

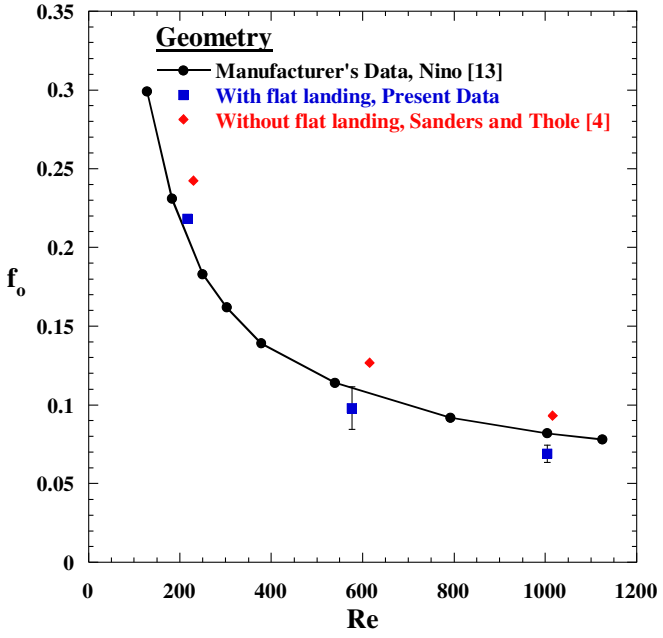

Fig. 9. Baseline friction factors measured between $0.73L_p$ up and downstream of the louvered fin array compared to a manufacturer's data. Uncertainty at $Re = 216$ was 51% of the measurement.

for comparisons to be made to data provided by a heat exchanger manufacturer [17] for an actual heat exchanger core. Fig. 9 presents the results of this comparison. Excluding the measured friction factor at $Re = 216$, which had high associated experimental uncertainty, measured friction factors for the geometry including the flat landings were slightly lower than the manufacturer's data. Note that the blockage of the tube wall increases pressure losses which would account for the higher friction factors measured by the manufacturer. Friction factor measurements were larger than the manufacturer's data for the geometry where no flat landing was included. This was due to the fact that when no landing was modeled, the flow path length was greater along the tube wall resulting in a larger pressure loss.

The remainder of this paper quantifies the effects of winglets and piercings on tube wall heat transfer and friction factor. The effects of winglet geometry and mirroring winglets across the turnover louver were studied using a solid louvered fin and will be reported. In addition, the mirrored winglet configurations that produced the highest heat transfer augmentations were further studied by including piercings into the louvered fin geometry.

8. Winglets on solid louvered fins with and without flat landings

Sanders [5] reported that winglets angled towards the tube wall produced small heat transfer augmentations when implemented into a louvered fin where no flat landing was modeled. Measurements showed a reduction in heat transfer (−3% with respect to the baseline) at $Re = 216$ with negligible positive augmentation (3%) at $Re = 955$. Conversely, incorporating winglets onto the flat landing of the more realistic scaled louvered fin geometry resulted in heat transfer augmentations of 1% and 47% at $Re = 216$ and 955, respectively. For $Re = 216$ the measured augmentation is within the experimental uncertainty. Fig. 10 compares the dramatic difference in winglets' influence on heat transfer performance for the different louvered fin geometries. Note that shown below the graph is a diagram of the winglet configuration used which was, $\alpha = 40°$, $\Lambda = 1.5$, $Z = 0.22$, with 28 winglets angled towards the wall in a non-mirrored configuration. As shown in Fig. 10, winglets on the louvered fins including flat landings increased average Nusselt number starting at the first winglet. Beginning at the turnover louver, on which there were no winglets, Nusselt numbers decreased before increasing again after the turnover where winglets were again implemented onto the louvered fin surfaces.

There are two physical mechanisms that lead to enhanced heat transfer along the tube wall from the use of winglets. The first of these mechanisms is the re-direction of cool freestream air towards the tube wall. The second mechanism is the formation of vortices by winglets that serve to enhance flow mixing and heat transfer along the tube wall.

The computational study of Lawson et al. [3] suggests that vortices produced by winglets in a louvered fin array where the flat landing is ignored are ineffective because

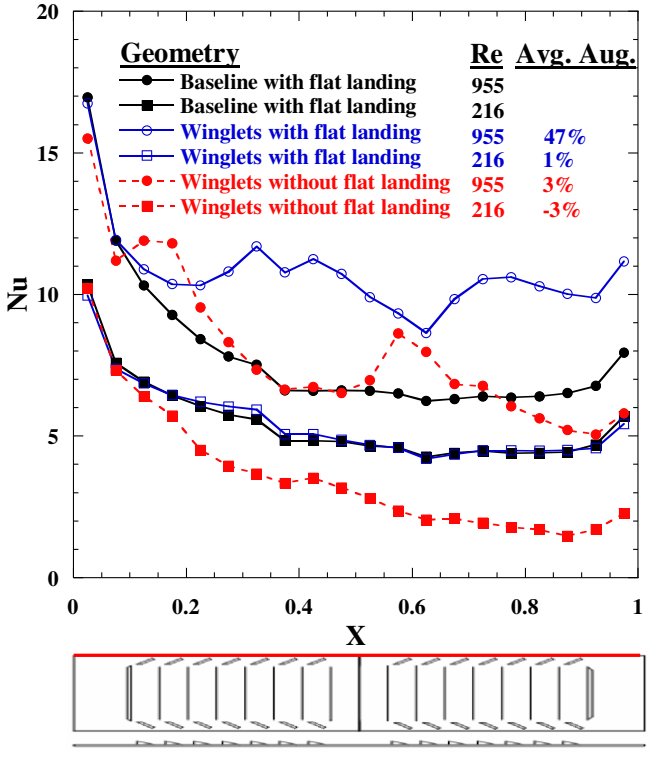

Fig. 10. Comparison of winglet heat transfer augmentation using louvered fin geometries with and without flat landings. Winglets without landing data from [4].

the vortices are disrupted by downstream louvers after only propagating a short distance in the streamwise direction. The computational predictions were made using the three-dimensional, steady flow solver in Fluent with the details given in Ref. [3]. The flow was considered to be laminar and periodic in the pitchwise direction. Fig. 11 demonstrates how winglets form vortices, but the vortices are unable to convect because of downstream louvers. In Fig. 11 the vortex can be seen forming as air rolls over the winglet from the pressure to the suction side, but is then disrupted as the vortex impacts the leading edge of the next louver in the streamwise direction. Conversely, for the geometry where the flat landing is modeled, vortices that are formed convect downstream in the channel-like flow without being disrupted by louvers.

These results suggest vortex propagation is the mechanism that caused the large augmentations in heat transfer. In a louver array where vortices are clearly formed, but not allowed to propagate, negligible augmentations were observed [3,5]. However, in the current study, delta winglets were placed in the region of channel-like flow allowing vortex propagation. This propagation caused the large heat transfer augmentations. It is likely that vortex interaction with the louver-directed flow caused increased convective transfer of the cooler louver-directed flow toward the hot tube wall leading to a reduction in air side resistance.

Both louvered fin geometries showed augmentations within the experimental uncertainty at $Re = 216$. Because of the low flow velocity at this Reynolds number, it is believed that winglets were unable to cause significant mixing. The trend of winglets producing negligible augmentations at $Re = 216$ was measured for all tests performed. This study found no winglet configuration that provided a Nusselt number augmentation larger than the experimental uncertainty at $Re = 216$.

The data clearly demonstrated that due to the different flow fields present for the different louvered fin geometries, ignoring the flat landing along the tube wall lead to an inaccurate assessment on the effect winglets had on heat transfer over the tube wall. To make measurements that will have practical significance in quantifying winglet effects on tube wall heat transfer, the three-dimensionality of the heat exchanger core should be considered. The remainder of this paper will focus on the geometry that modeled the flat landing along the tube wall.

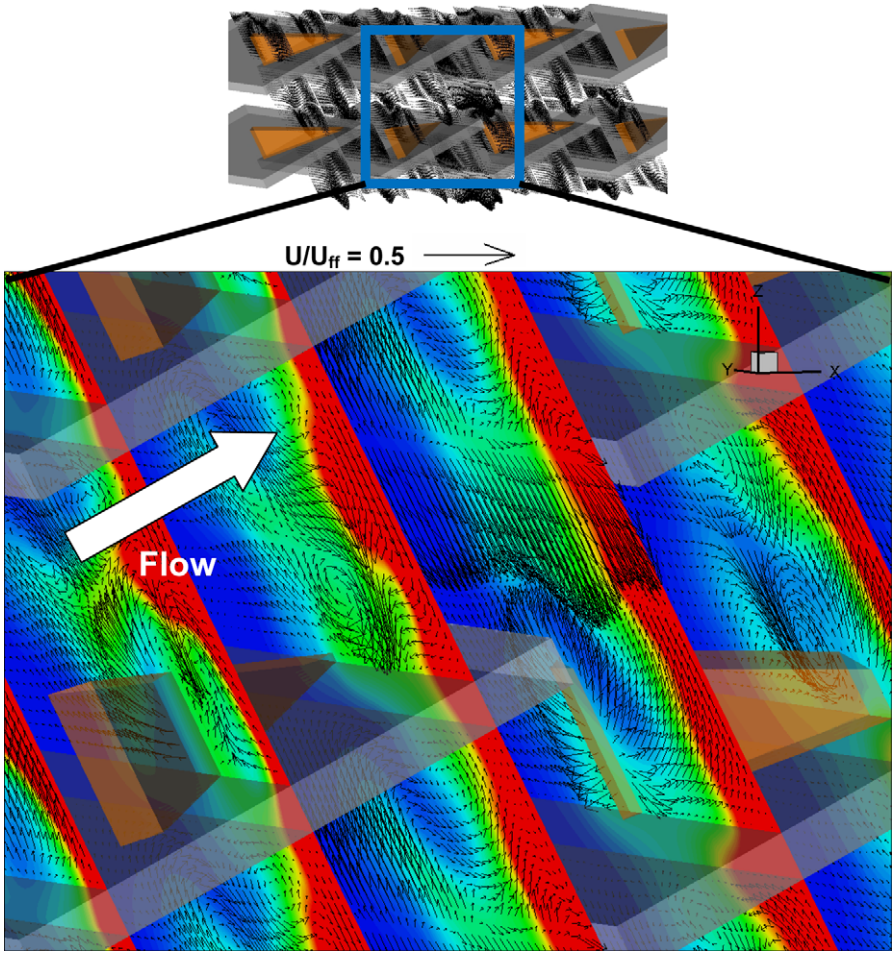

Fig. 11. Secondary flow vectors showing a winglet forming a vortex in a louvered fin array without flat landings. Flow is from left to right following the louver direction [3].

9. Mirrored and non-mirrored winglet configurations on solid louvered fins

During the assembly of heat exchanger cores, a louvered fin array incorporating winglets can be placed in several orientations. For a winglet configuration to be of practical use in a heat exchanger, the configuration should provide performance enhancements that are independent of the flow direction relative to the louvers. To simulate this in our experiments, the winglet setup was mirrored downstream of the turnover louver. Fig. 5 illustrates the definition of mirroring winglets across the turnover louver.

Heat transfer measurements, as shown in Fig. 12, indicated mirroring the winglet setup decreased Nusselt number augmentations compared to a non-mirrored winglet configuration. The non-mirrored configuration produced average augmentations of 47%, 30%, and 1%, while the mirrored configuration caused average augmentations of 33%, 14%, and −5% at $Re = 955$, 577, and 216, respectively. Before the turnover louver where winglets were angled at the wall, the non-mirrored and mirrored configurations performed similarly. Fig. 13 shows the Nusselt number augmentation at each measurement location along the tube wall. At $X = 0.6$, which was the location of the first winglet angled away from the wall in the mirrored configuration, the augmentation decreased.

The large decrease in augmentation, which started at $X = 0.6$, is clearly due to the delta winglets being angled away from the wall. Winglets angled away from the wall

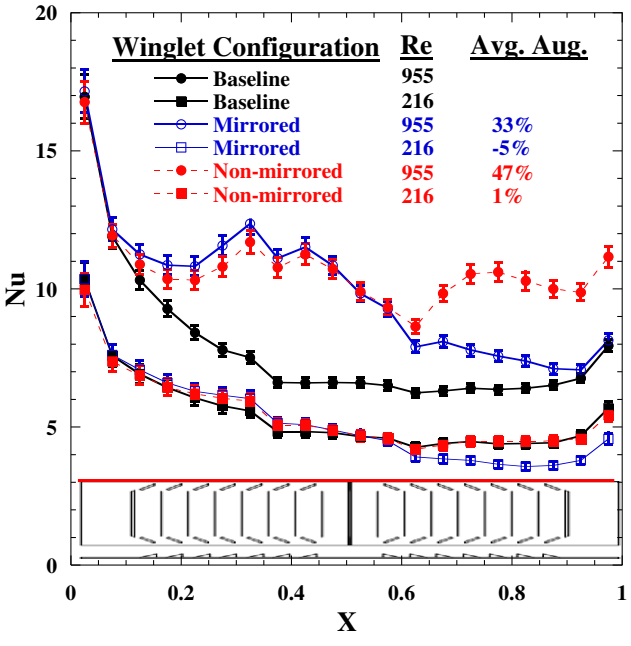

Fig. 12. Comparison of heat transfer performance between non-mirrored and mirrored winglet configurations. Parameters for these tests were: $\alpha = 40°$, $\Lambda = 1.5$, $t_w = t$ using 28 winglets. For the non-mirrored test $Z = 0.22$, and for the mirrored test $Z = 0.15$. Note that the winglet setup shown is for the mirrored configuration. Representative uncertainty bars are shown for local Nusselt number measurements.

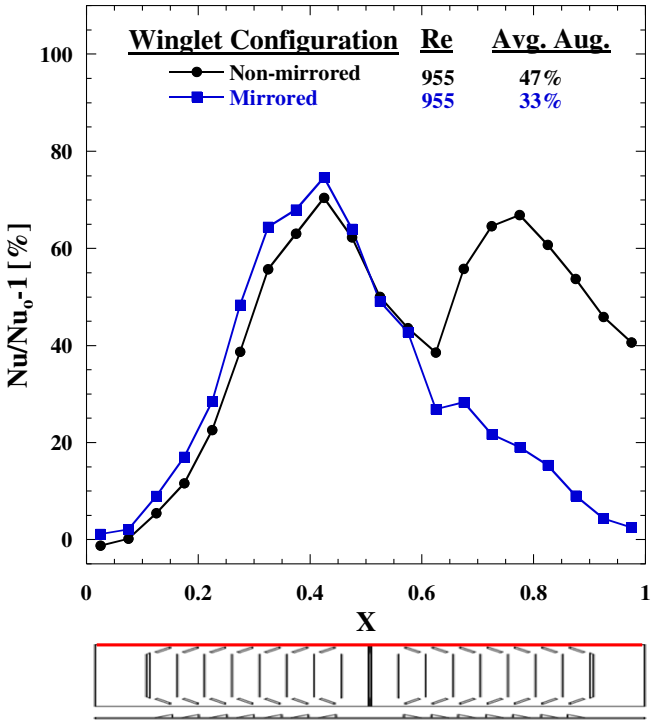

Fig. 13. Nusselt number augmentations along the tube wall for non-mirrored and mirrored winglet configurations at $Re = 955$. Parameters for the tests were the same as Fig. 12.

formed vortices rotating in the opposite direction from the vortices formed by winglets angled towards the wall. This change in vortex rotation direction did not increase the mixing of louver-directed flow with the channel flow. It decreased it because vortex propagation was temporally interrupted. These effects lead to the lower heat transfer augmentation of mirrored winglet configurations.

Non-mirrored and mirrored winglet configurations showed only small differences in friction factor performance. The non-mirrored configuration increased friction factor measurements by 19%, while the mirrored configuration showed a 25% increase at $Re = 955$. This was expected as half the winglets in the mirrored case had the large winglet end facing upstream, which has been determined by Sanders [5] to cause larger pressure losses than winglets with the shorter end facing upstream.

Mirroring the winglet configuration across the turnover louver negatively affected winglet performance; however, augmentations of up to 33% in heat transfer were still achieved. Although non-mirrored winglet configurations showed higher heat transfer augmentations with lower increases in friction factor, the remainder of the results reported in this study will be for mirrored winglet configurations in an attempt to present results relevant to an assembled heat exchanger.

10. Winglet geometry effects tested on solid louvered fins

Sanders and Thole [4] demonstrated that the winglet aspect ratio and distance from tube wall affected heat

transfer performance for a louvered fin geometry where the louvers spanned the entire fin height (no flat landing). It is important to note that the winglet aspect ratio is a ratio of winglet height to the base, where aspect ratio decreases with winglet size because the winglet height is fixed. It was shown that the effect of winglets on tube wall heat transfer was different depending on if the flat landing along the tube wall was simulated. Therefore, the effects of varying winglet aspect ratio and distance from the tube wall were measured using the scaled louvered fin geometry which included the flat landing. Aspect ratio and distance from tube wall both affected Nusselt number measurements as shown by Figs. 14 and 15.

As seen in Fig. 14, Nusselt number augmentations increased with decreasing aspect ratio. At $Re = 955$, the measured augmentation averages were 24%, 28%, and 33% for aspect ratio's of 3, 2, and 1.5, respectively. On flat plates, the vortex strength has been observed to be dependent on the winglet aspect ratio with smaller aspect ratio winglets forming stronger vortices. Consistent with flat plate results, increases in Nusselt number augmentations with decreasing aspect ratio occurred because smaller aspect ratio winglets formed stronger vortices that increased disruption of the tube wall boundary layer. Due to the blockages of larger winglets, friction factors also increased with decreasing aspect ratio from 11% for $A = 3$–22% for $A = 1.5$ at $Re = 955$.

Fig. 15 clearly shows that as winglets were placed closer to the tube, Nusselt number augmentations increased. At $Re = 955$ for $Z = 0.15$, 0.22, and 0.29, augmentation averages were 33%, 33% and 31%, respectively. While increases were seen in augmentations with decreasing winglet distance from the tube wall, there was only a 2.3% difference between the highest and lowest augmentations observed at $Re = 955$. Winglet placement influenced the position of vortices with respect to the tube wall. Vortex strength and not location were shown by Gentry and Jacobi [11] to be the more dominant factor influencing heat transfer. The results of the winglet distance from tube wall tests agreed with Gentry and Jacobi's [11] findings as distance from tube wall was shown to be a minor effect on heat transfer augmentation. Similarly, varying winglet distance from the tube wall was shown to have negligible effects on friction factor. Friction factor increases varied between 22% and 24% for $Z = 0.22$ and 0.15, respectively at $Re = 955$, which was within the experimental uncertainty.

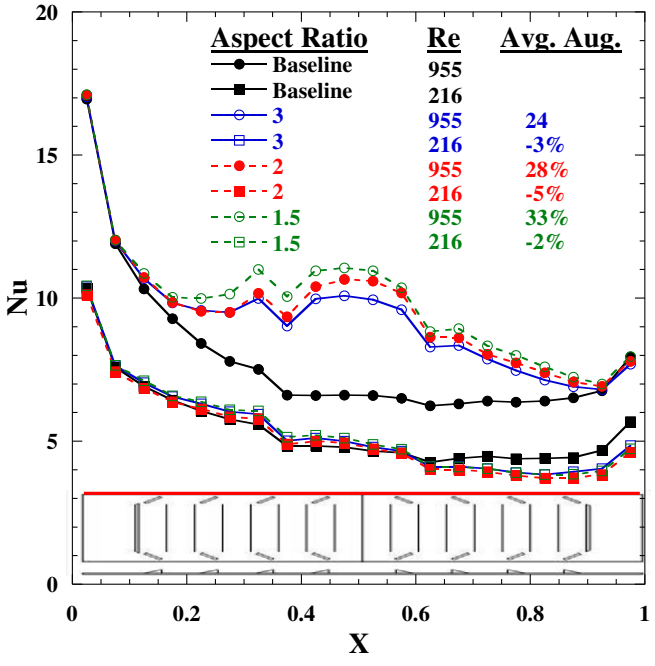

Fig. 14. Comparison of heat transfer performance between winglets configurations of different aspect ratios. Parameters for the tests were: $\alpha = 40°$, $Z = 0.22$, $t_w = 0.03t$, using 16 winglets.

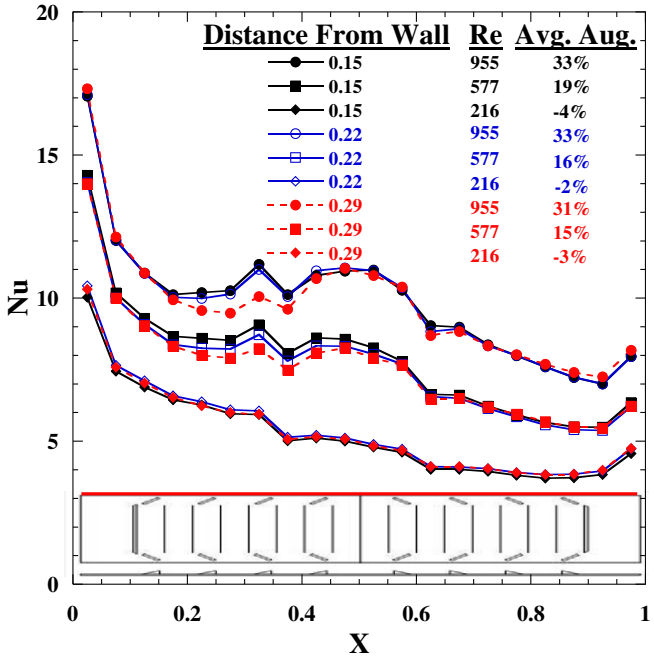

Fig. 15. Comparison of heat transfer performance between winglet configurations having different distances from the tube wall. Parameters for the tests were: $\alpha = 40°$, $A = 1.5$, $t_w = 0.03t$, using 16 winglets.

The experiments for determining the effects of varying winglet aspect ratio and distance from tube wall were performed using a winglet thickness of $0.03t$. Pierced louver testing was performed using winglets having a winglet thickness equal to the louver thickness, which is representative of winglets that can be manufactured. To determine if the same Nusselt number trends would result from using thick winglets, the effect of winglet thickness on heat transfer performance was measured. Fig. 16 presents measured Nusselt numbers for thick and thin winglet configurations. The average Nusselt number augmentations were nearly the same and, more importantly, trends were the same. These data indicated that winglet thickness was also not a significant variable.

Maintaining the structural integrity of louvered fins is an important consideration. As such, we considered the effects of varying the number of winglets placed on the louvered fins. To determine if winglet performance was better

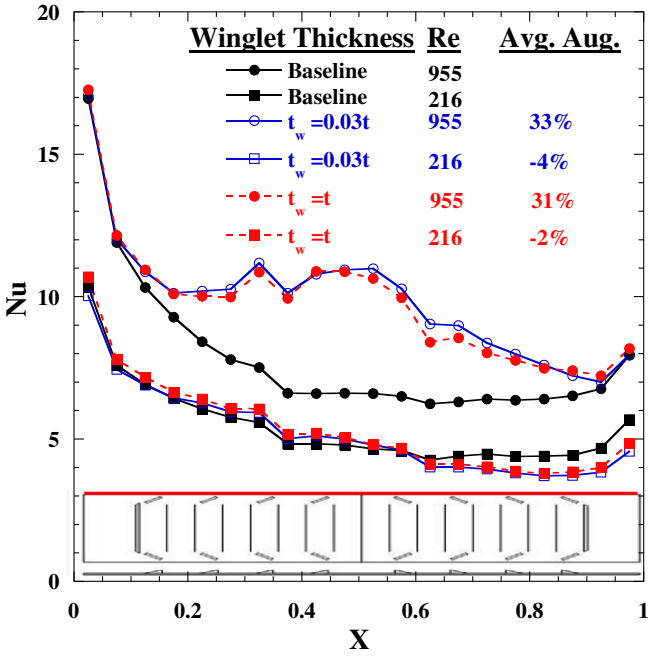

Fig. 16. Comparison of heat transfer performance between winglet configurations having different winglet thicknesses. Parameters for tests were: $\alpha = 40°$, $\Lambda = 1.5$, $Z = 0.15$, using 16 winglets.

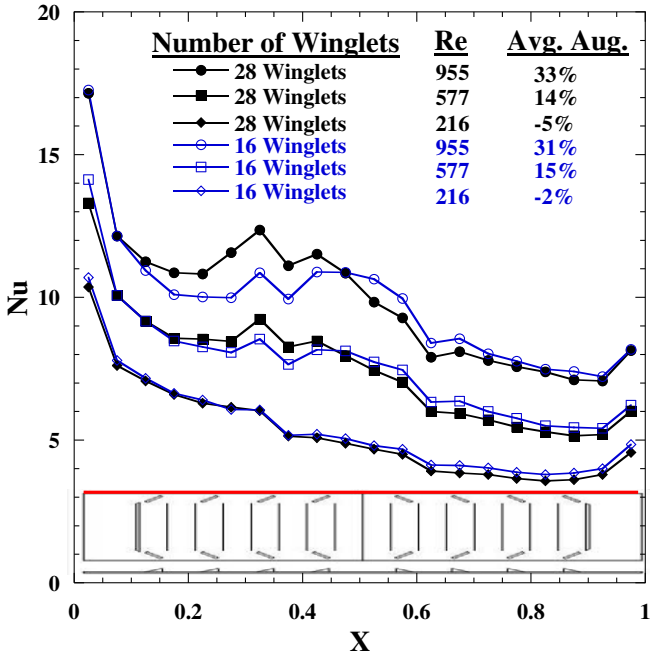

Fig. 17. Comparison of heat transfer performance between 28 and 16 winglet configurations. Parameters for the tests were: $\alpha = 40°$, $\Lambda = 1.5$, $Z = 0.15$, and $t_w = t$. Note that the winglet configuration diagram shown is for the 16 winglet configuration.

for 16 or 28 winglet configurations, a comparison was performed. Fig. 17 presents the Nusselt number data measured for the 16 versus 28 winglet comparison tests. There was negligible (within experimental uncertainty) difference between the 16 and 28 winglet configurations with only a 2% difference in Nusselt number augmentation at $Re = 955$ and a 1% (14% and 15% for the 28 and 16 winglet configurations, respectively) difference at $Re = 577$. Fig. 17 shows the 28 winglet configuration provided a significant advantage over the 16 winglet configuration in augmenting Nusselt number before the turnover louver for $Re = 955$. The overall advantage of the 28 winglet configuration is decreased after the turnover, where the 16 winglet configuration provided higher Nusselt number augmentations. The 28 winglet configuration performed worse than the 16 winglet configuration after the turnover louver because it had more winglets angled away from the wall. Friction factor measurements indicated no difference between 16 and 28 winglet configurations with both having a 25% increase in friction factor at $Re = 955$.

11. Effects of simulated piercings

Based on the findings of the solid louvered fin tests, two winglet geometries were chosen to test the effect of piercings on winglet performance. The two winglet configurations chosen differed only in the aspect ratio of the winglets used. Winglets with $\Lambda = 1.5$ were selected because these were observed to produce the highest heat transfer augmentation in solid louvered fin testing. Minimizing the piercing area was an important consideration because any area removed from the louvered fin would decrease the fin's structural integrity. Also the area available for heat conduction from the tube wall through the louvered fins would be decreased. For this reason, $\Lambda = 2$ winglets were tested as piercing area decreased with increasing winglet aspect ratio.

Fig. 18 indicates piercings reduced the Nusselt number augmentation produced by winglets. The highest augmentations measured for the pierced louvered fin configurations were 24% and 8%,which corresponds to a 11% and 9% reduction in heat transfer compared to the same solid louvered fin winglet configuration at $Re = 955$ and 577, respectively. Measured reductions in heat transfer augmentation occurred only before the turnover louver where winglets were angled towards the tube wall. After the turnover louver where winglets were angled away from the wall there were no negative effects of piercings. Incorporating piercings increased Nusselt number augmentation after the turnover louver. The decreased augmentation from the piercings was caused by flow ingestion through the piercings. Smoke visualization showed that when piercings were implemented into the louvered fin geometry, flow over the flat landings near the tube wall no longer resembled channel-like flow. Piercings provided a flow path that allowed the flow along the tube wall to more closely follow the louver-directed flow. The flow through the piercings also disrupted the vortex formation, which decreased the ability of winglets to augment heat transfer. This suggests that the vortices formed were susceptible to even small disturbances in the flow along the tube wall.

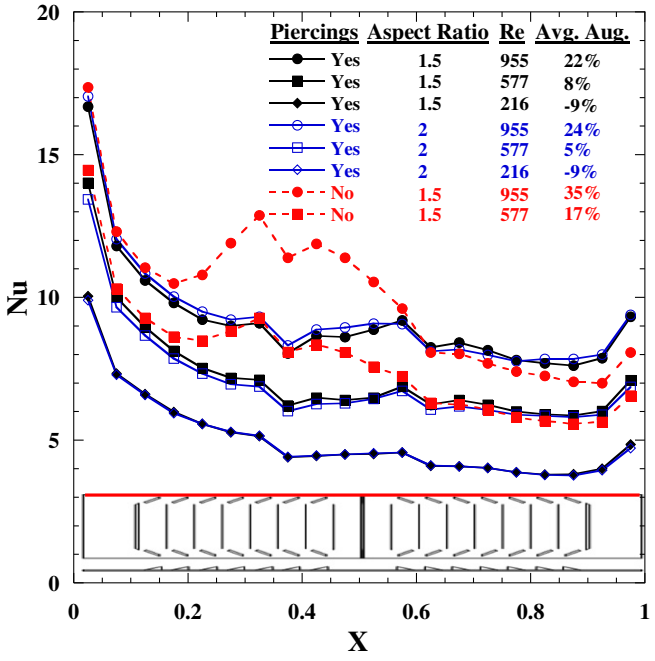

Fig. 18. Comparison of heat transfer performance between pierced and solid fin winglet configurations. Parameters for the tests were: $\alpha = 30°$, $Z = 0.15$, $t_w = t$, using 28 winglets.

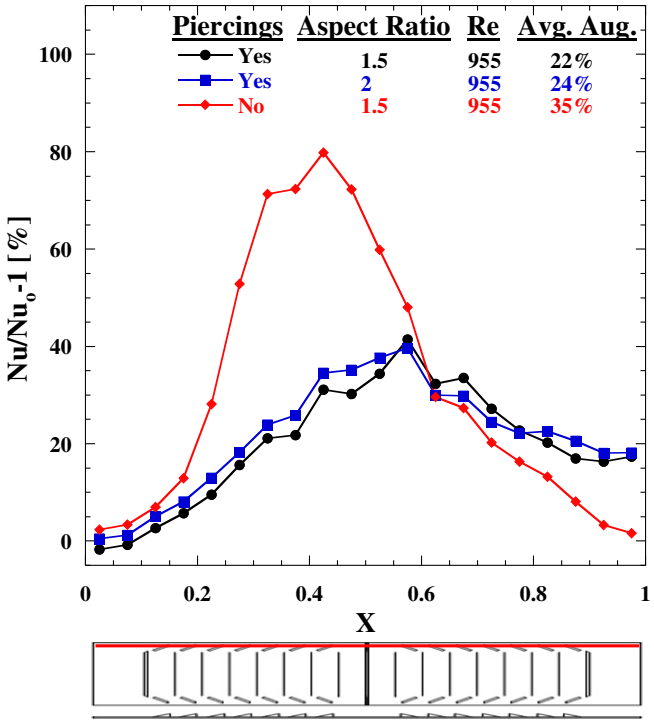

Fig. 19. Nusselt number augmentations for pierced and solid louvered fin configurations at $Re = 955$. Parameters for the tests were: $\alpha = 30°$, $Z = 0.15$, $t_w = t$, using 28 winglets.

In the solid louvered fin tests, decreasing winglet aspect ratios was consistently shown to increase Nusselt number augmentation. With pierced louvered fins, smaller aspect ratio winglets had larger piercings and allowed more flow to be ingested. As can be seen by comparing Figs. 14 and 18, smaller piercings of $\Lambda = 2$ winglets resulted in larger Nusselt number augmentations than $\Lambda = 1.5$ winglets at $Re = 955$. Although smaller aspect ratio winglets created stronger vortices and redirect more air towards the tube wall, these effects were offset by more flow passing through the large $\Lambda = 1.5$ piercings.

Augmentation results at each measurement location for the pierced and solid louvered fins, shown in Fig. 19, indicated that before the turnover louver, winglets with $\Lambda = 2$ produced higher augmentations than $\Lambda = 1.5$ winglets. After the turnover louver the larger $\Lambda = 1.5$ winglets produced higher Nusselt number augmentations than $\Lambda = 2$ winglets. It was also interesting to observe that negative effects of piercings only occurred before the turnover louver, where the winglets were angled towards the tube wall. After the turnover louver, where winglets were angled away from the wall, piercings increased Nusselt number augmentation compared to the solid louvered fins. It was shown previously that winglets angled away from the tube wall direct air away from the wall decreasing the Nusselt number augmentation. Piercings interfered with the winglet influence causing the larger Nusselt number augmentations after the turnover louver for the pierced louvered fin configurations. Flow passing through the piercings also explains why $\Lambda = 1.5$ winglets with the largest piercings outperformed $\Lambda = 2$ winglets after the turnover louver. The piercings of the $\Lambda = 1.5$ winglets provided a larger flow path than piercings for the $\Lambda = 2$ winglets. As such, the $\Lambda = 1.5$ winglets did not direct as much air away from the tube wall as the $\Lambda = 2$ winglets did, causing the $\Lambda = 1.5$ winglets to perform better after the turnover louver.

Friction factor tests indicated that piercings decreased the friction factors through the test section relative to the solid louvered fin configuration. The solid louvered fin configuration produced friction factor increases of 25% over the baseline, while the pierced louvered fin configurations had only 18% and 10% for $\Lambda = 1.5$ and 2, respectively at $Re = 955$. Flow through the piercings caused less shear at the interface between the louver-directed flow and channel-directed flow regimes. The reduction in shear between the regions of channel flow and louver-directed flow accounted for the measured decrease in friction factor relative to the solid louver.

12. Conclusions

This study investigated the use of delta winglets as a means to increase tube wall heat transfer in louvered fin heat exchangers. Tests were performed using a scaled louvered fin geometry that accurately modeled the flat landing along the tube wall onto which delta winglets and winglet piercings were incorporated. By comparing the results to past studies which used a simplified louvered fin geometry where the flat landing was ignored, it was demonstrated that the three-dimensionality of louvered fins and the transition

between the louvers and the tube wall must be accounted for to make accurate tube wall heat transfer measurements.

For a geometry neglecting the flat landings, Sanders [5] found that delta winglets angled towards the tube wall produced 3% Nusselt number augmentation at a Reynolds number of 955. When the flat landings were modeled, the same winglet configuration was found to give a 47% Nusselt number augmentation at the same Reynolds number. The mechanism causing heat transfer augmentation for winglets placed on the flat landings was vortices sweeping the tube wall surface. Conversely, when winglets were placed on louvers that spanned the entire fin, the vortices formed were disrupted by downstream louvers.

Piercings in the louvered fins decreased the benefits of winglets on augmenting heat transfer. Piercings disrupted the vortex formation by allowing flow to pass through the piercings and follow the louver-directed flow path. While piercings were shown to negatively affect heat transfer performance along the tube wall relative to winglets placed on solid louvered fins, they have the desirable effect of lowering pressure losses.

It is important to note that heat transfer augmentations reported in this paper only take into account heat transfer along the tube wall surface. Winglets with piercings will also have effects on louver heat transfer. For example, the flat landings near the tube wall that are swept by vortices would have likely shown increases in heat transfer. Another effect of incorporating winglets and piercing into louvered fin designs is a decrease in the area available for heat conduction from the tube wall through the louvered fins. This area reduction could possibly cause a decrease in louver heat transfer.

Overall, this study found that delta winglets including simulated piercings are a promising means of augmenting heat transfer in louvered fin heat exchangers, providing up to 24% augmentation over the tube wall surface. For a final conclusion to be reached on the practicality of implementing delta winglets into louvered fin heat exchanger designs, overall heat exchanger performance must be measured where all winglet and piercing effects are accounted for using a realistic louvered fin geometry.

Acknowledgements

The authors would like to acknowledge Modine Manufacturing Inc. for their support on this project. In particular the authors would like to thank Drs. Victor Nino and Steve Memory who have provided technical feedback for this work.

References

[1] Yu-Juei Chang, Kuei-Chang Hsu, Yur-Tsai Lin, Chi-Chuan Wang, A generalized friction correlation for louver fin geometry, Int. J. Heat Mass Transfer 43 (12) (2000) 2237–2243.

[2] Yu-Juei Chang, Chi-Chuan Wang, A generalized heat transfer correlation for louver fin geometry, Int. J. Heat Mass Transfer 40 (3) (1997) 533–544.

[3] M.J. Lawson, P. Sanders, K.A. Thole, A computational and experimental comparison of tube wall heat transfer augmented by winglets in louvered fin heat exchangers, in: International Mechanical Engineering Congress and Exhibition, Chicago, IL, 2006, Paper number 14452.

[4] P. Sanders, K.A. Thole, Effects of winglets to augment tube wall heat transfer in louvered fin heat exchangers, Int. J. Heat Mass Transfer 49 (21–22) (2006) 4058–4069.

[5] P. Sanders, Effects of louver length and vortex generators to augment tube wall heat transfer in louvered fin heat exchangers, MSME Thesis, Virginia Tech, Blacksburg, VA, 2005.

[6] F.N. Beauvais, An aerodynamic look at automotive radiators, SAE Transactions 74, 1966, Paper number 650470.

[7] C.J. Davenport, Heat transfer and flow friction characteristics of louvered heat exchanger surfaces, in: J. Taborek (Ed.), Heat Exchangers: Theory and Practice, Hemisphere/McGraw-Hill, Washington, DC, 1983, pp. 397–412.

[8] K.N. Atkinson, R. Draulic, M.R. Heikal, T.A. Cowell, Two- and three-dimensional numerical models of flow and heat transfer over louvered fin arrays in compact heat exchangers, Int. J. Heat Mass Transfer 41 (24) (1998) 4063–4080.

[9] D.K. Tafti, J. Cui, Fin-tube junction effects on flow and heat transfer in flat tube multilouvered heat exchangers, Int. J. Heat Mass Transfer 46 (11) (2003) 2027–2038.

[10] G. Biswas, K. Torii, D. Fujii, K. Nishino, Numerical and experimental determination of flow structure and heat transfer effects of longitudinal vortices in a channel flow, Int. J. Heat Mass Transfer 39 (16) (1996) 3441–3451.

[11] M.C. Gentry, A.M. Jacobi, Heat transfer enhancement by delta-wing-generated tip vortices in flat plate and developing channel flows, J. Heat Transfer Trans. ASME 124 (6) (2002) 1158–1168.

[12] M.L. Smotrys, H. Ge, A.M. Jacobi, J.C. Dutton, Flow and heat transfer behavior for a vortex-enhanced interrupted fin, J. Heat Transfer 125 (2003) 788–794.

[13] A. Joardar, A.M. Jacobi, Impact of leading edge delta-wing vortex generators on the thermal performance of a flat tube louvered-fin compact heat exchanger, Int. J. Heat Mass Transfer 48 (8) (2005) 1480–1493.

[14] V. Prabhakar, G. Biswas, V. Eswaran, Numerical prediction of heat transfer in a channel with a built-in oval tube and two different shaped vortex generators, Numer. Heat Transfer: Part A, Applicat. 41 (3) (2002) 307–329.

[15] A. Jain, G. Biswas, D. Maurya, Winglet type vortex generators with common-flow-up configuration for fin-tube heat exchangers, Numer. Heat Transfer: Part A, Applicat. 43 (2) (2003) 201–219.

[16] R. Vasudevan, V. Eswaran, G. Biswas, Winglet-type vortex generators for plate fin heat exchangers using triangular fins, Numer. Heat Transfer 38 (5) (2000) 533–555.

[17] V.G. Nino, Personal communication through Modine Manufacturing, 2006.

[18] C. Ebeling, K.A. Thole, Measurements and predictions of the heat transfer at the tube-fin junction for louvered fin heat exchangers, Int. J. Compact Heat Exchangers 5 (2004) 265–286.

[19] A.C. Lyman, R.A. Stephan, K.A. Thole, L. Zhang, S. Memory, Scaling of heat transfer coefficients along louvered fins, Exp. Therm. Fluid Sci. 26 (5) (2002) 547–563.

[20] R.A. Stephan, K.A. Thole, Optimization study relevant to louvered fin heat exchangers, Int. J. Heat Exchangers 6 (1) (2005) 73–92.

[21] M.E. Springer, K.A. Thole, Experimental design for flowfield studies of louvered fins, Exp. Therm. Fluid Sci. 18 (3) (1998) 258–269.

[22] M.F. Modest, Radiative Heat Transfer, second ed., Academic Press, New York, 2003, pp. 762–773.

[23] F.M. White, Fluid Mechanics, fifth ed., McGraw-Hill, New York, 2003, pp. 384–393.

[24] R.J. Moffat, Describing the uncertainties in experimental results, Exp. Therm. Fluid Sci. 1 (1988) 3–17.